



Study of beam-beam effects with offset and angle scans

I.-A. Melzer-Pellmann*

June 19, 2007

Abstract

Luminosity is sensitive to both vertical beam-beam offset and crossing angle. Therefore, some luminosity loss is also expected from internal bunch deformations like those induced by single-bunch wakefields in the linac ('banana effect'). This effect is studied for different ILC parameter sets using a simulation of a single bunch correlated emittance growth of 6% in average. This study shows that the effect of beam-beam interactions are small in offset and angular displacements and that the the luminosity loss due to the banana effect can be compensated by an offset correction followed by an angular correction of the beams.

*DESY, Hamburg, Germany

1 Introduction

In the TESLA TDR [1] it was shown that, with the chosen beam parameters, the luminosity is very sensitive to both vertical beam-beam offset and crossing angle. It was also shown that the luminosity loss due to internal bunch deformations, such as those induced by single-bunch wakefields in the linac could be partly compensated by taking advantage of the sensitivity of the luminosity to offset and angle.

These effects are studied here again for different ILC parameter sets, [2] shown in tables 1 and 2, using the beam-beam simulation GUINEA-PIG [3].

2 Vertical and angular scans

2.1 Offset scans for ILC parameters

The sensitivity to an offset displacement was investigated for the different ILC parameters and energies. The expected relative luminosity loss vs. the offset normalised to the beam size σ_y is shown in Fig. 1. It is similar for the different ILC parameters and of the same order of magnitude as the expected loss without beam-beam interaction, calculated with the following formula:

$$\mathcal{L}/\mathcal{L}_{NOM} = e^{-\frac{1}{4}\sigma_y^2}$$

The absolute luminosity values for zero offset and angle are summarized in table 3.

2.2 Angle scans for ILC parameters

The sensitivity to an angular displacement was studied in the same way for the different ILC parameters. Figure 2 shows that the relative luminosity loss vs. the angle normalized to the transverse bunch divergence $\Theta_y = \sqrt{\epsilon_y/\beta_y}$. The luminosity loss is minimal for the LOWQ (low bunch charge) option ($\approx 86\%$ for $\alpha_y/\Theta_y = 1$) and largest for the LARGEY (increased vertical beam size) option ($\approx 58\%$ for $\alpha_y/\Theta_y = 1$). This effect can be explained by the different strength of beam disruption in the vertical plane (D_y), which is smallest for the LOWQ and largest for the LARGEY option (shown in tables 1 and 2).

2.3 Offset followed by angle scans with correlated emittance growth

Due to the above shown sensitivity to offset and angular displacement of the beams, some luminosity loss is expected from internal bunch deformations like those induced by single-bunch wakefields in the linac ('banana effect'). For TESLA the single-bunch correlated emittance growth is expected to be 6% in average [1]. This number was also used here to test the effect for the ILC parameters. Figures 3 - 7 show that for all parameter sets it is possible to reobtain nearly the full luminosity by doing an offset scan followed by an angle scan for the offset value with the highest luminosity. Furthermore, the effect is smaller for the ILC parameters than for the previously studied TESLA parameters.

3 Conclusion

It is shown that the effect of beam-beam interactions in offset displacements are small for the different ILC parameter sets. For the TESLA parameters, this effect was about twice larger. The luminosity loss due to angular displacement is dependent on the chosen ILC parameter set. Compared to the TESLA parameters, it's of the same order of magnitude for the LARGEY and LOWP option, and about a factor of three smaller for the LOWQ option. Furthermore, the effect of single-bunch wakefields in the linac is studied using a simulation of a single-bunch correlated emittance growth of 6% in average. The small luminosity loss due to this 'banana effect' can be compensated by an offset correction followed by an angular correction of the beams.

Acknowledgement

This work is supported by the Commission of the European Communities under the 6th Framework Programme "Structuring the European Research Area", contract number RIDS-011899.

References

- [1] R. D. Heuer, D. Miller, F. Richard, P. Zerwas (eds.), "TESLA Technical Design Report, Part II", DESY 2001-011, ECFA 2001-209, 2001.
- [2] T. Raubenheimer, "Suggested ILC Beam Parameter Range, Rev. 2/28/05", [http://www-project.slac.stanford.edu/ilc/acceldev/beampar/Suggested ILC Beam Parameter Space.pdf](http://www-project.slac.stanford.edu/ilc/acceldev/beampar/Suggested%20ILC%20Beam%20Parameter%20Space.pdf).
- [3] D. Schulte, DESY-TESLA-97-08.

	Nominal	Low Q	Large Y	Low P	High Lumi	TESLA
E_{CMS}/GeV	500	500	500	500	500	500
$N_{Particle} / 10^{10}$	2	1	2	2	2	2
N_{Bunch}	2820	5640	2820	1330	2820	2820
$\gamma\epsilon_x / \mu\text{m}\cdot\text{rad}$	10	10	12	10	10	10
$\gamma\epsilon_y / \mu\text{m}\cdot\text{rad}$	0.04	0.03	0.08	0.035	0.03	0.03
β_x / mm	21	12	10	10	10	15
β_y / mm	0.4	0.2	0.4	0.2	0.2	0.4
σ_x / nm	655	495	495	452	452	554
σ_y / nm	5.7	3.5	8.1	3.8	3.5	5.0
$\sigma_z / \mu\text{m}$	300	150	500	200	150	300
D_x	0.162	0.0708	0.468	0.226	0.170	0.226
D_y	18.5	10.0	28.6	27.0	21.9	25.3

Table 1: Beam and IP parameters for 500 GeV cms for different ILC options compared to the TESLA parameters.

	Nominal	Low Q	Large Y	Low P	High Lumi	TESLA
E_{CMS}/GeV	1000	1000	1000	1000	1000	800
$N_{Particle} / 10^{10}$	2	1	2	2	2	1.4
N_{Bunch}	2820	5640	2820	1330	2820	4886
$\gamma\epsilon_x / \mu\text{m}\cdot\text{rad}$	10	10	12	10	10	8
$\gamma\epsilon_y / \mu\text{m}\cdot\text{rad}$	0.04	0.03	0.08	0.035	0.03	0.015
β_x / mm	30	15	11	12	10	15
β_y / mm	0.3	0.2	0.6	0.2	0.2	0.4
σ_x / nm	554	392	367	350	320	392
σ_y / nm	3.5	2.5	7.0	2.7	2.5	2.8
$\sigma_z / \mu\text{m}$	300	150	600	200	150	300
D_x	0.113	0.0567	0.509	0.189	0.170	0.198
D_y	17.9	8.96	26.7	24.7	21.9	28.0

Table 2: Beam and IP parameters for 1000 GeV cms for different ILC options compared to the TESLA parameters.

	Nominal	Low Q	Large Y	Low P	High Lumi
$\mathcal{L}/10^{34} \text{ cm}^{-2} \text{ s}^{-1} (E_{CMS} = 500 \text{ GeV})$	2.07	1.99	1.73	2.01	5.11
$\mathcal{L}/10^{34} \text{ cm}^{-2} \text{ s}^{-1} (E_{CMS} = 1000 \text{ GeV})$	3.42	3.49	3.20	3.60	10.34

Table 3: Absolute luminosity values for caculated with GUINEA-PIG.

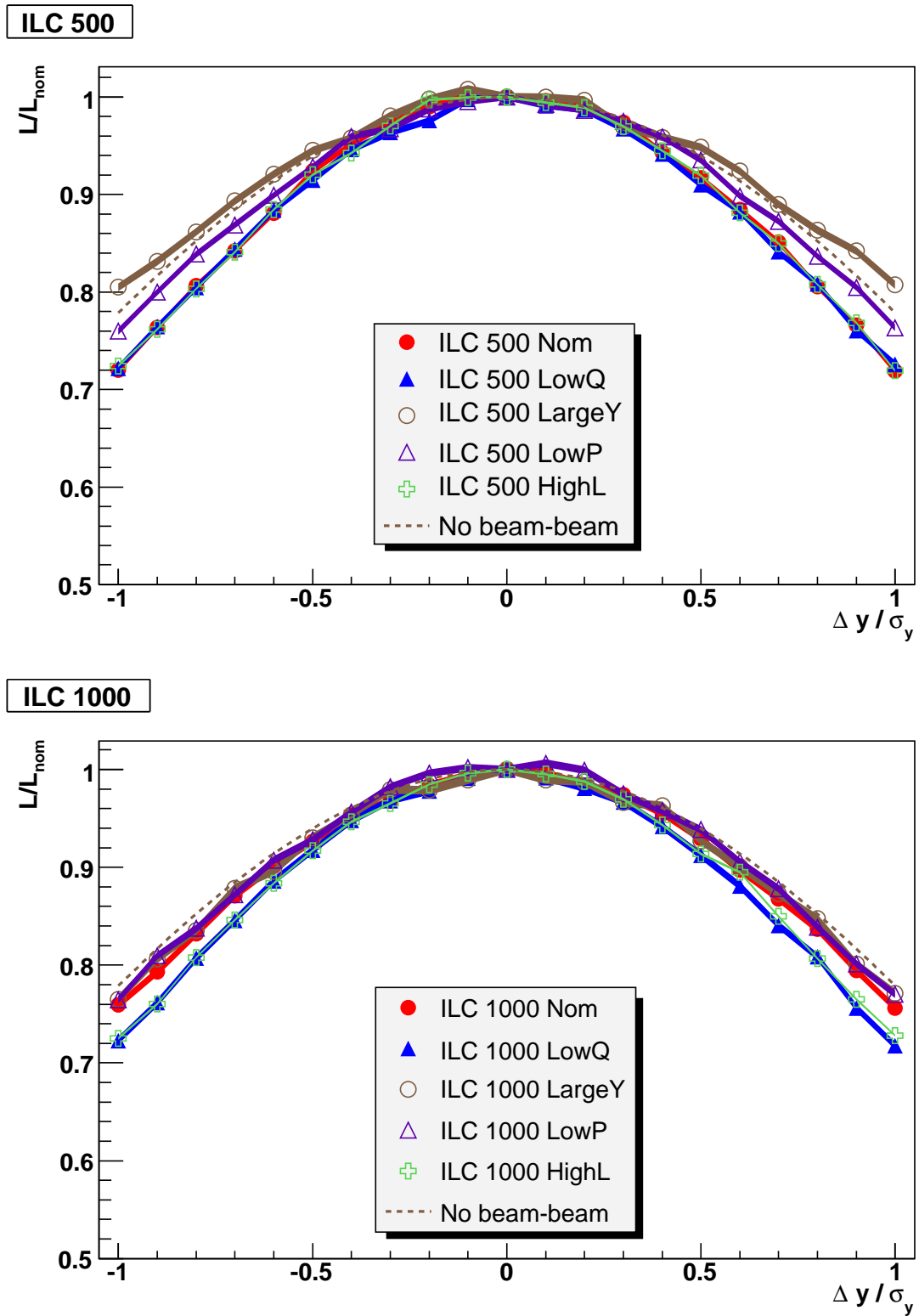


Figure 1: Normalized luminosity loss as a function of normalised IP vertical offset for the different ILC parameters for 500 and 1000 GeV compared to the luminosity loss for no beam-beam interaction.

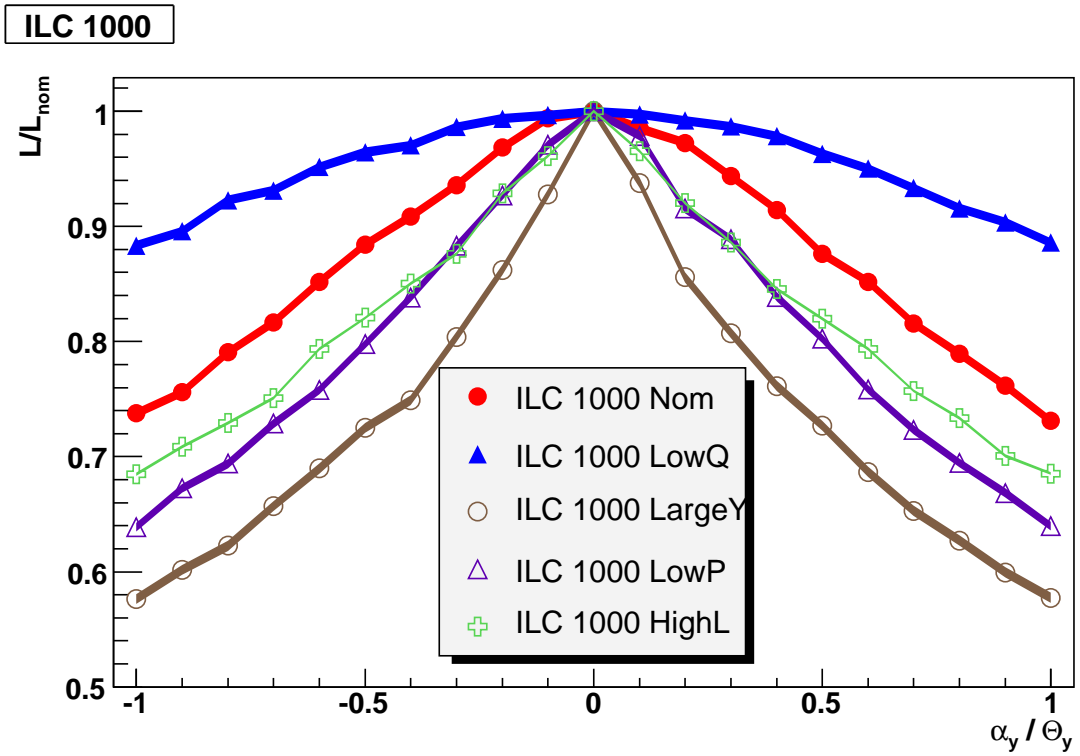
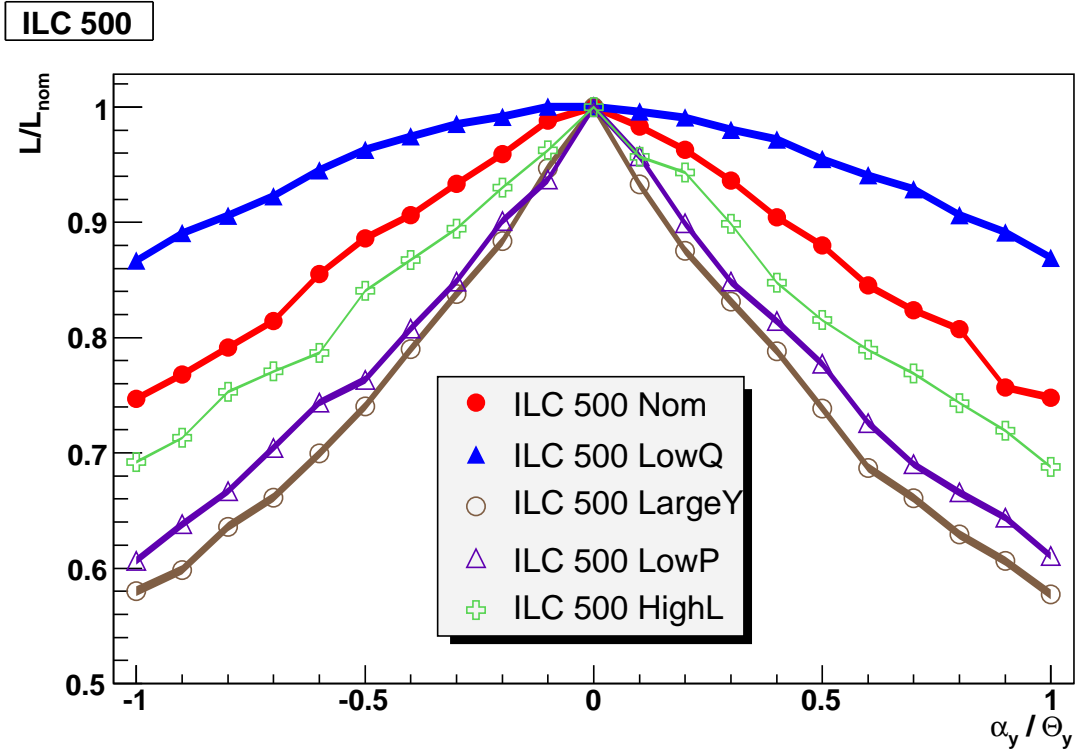


Figure 2: Normalized luminosity loss as a function of normalised IP angular offset for the different ILC parameters for 500 and 1000 GeV.

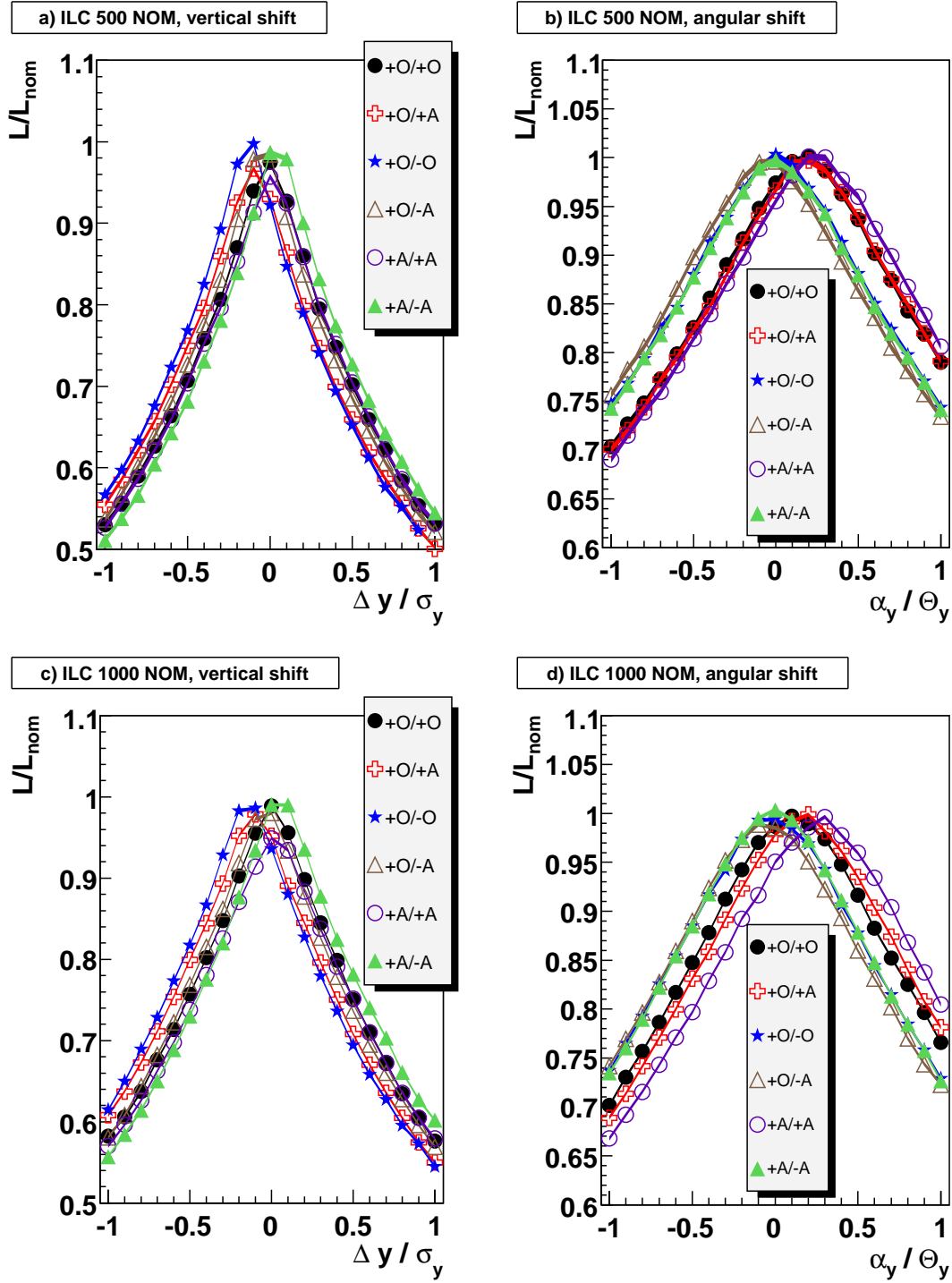


Figure 3: Offset followed by angle scans of the normalised luminosity for different combinations of vertical (O = offset (y-plane)) to angular (A = angle (y'-plane)) correlations leading to 6 % luminosity growth. The angle scans have been performed for the maximum luminosity reached in the offset scan. Shown here is the nominal option for 500 GeV (a and b) and 1000 GeV (c and d).

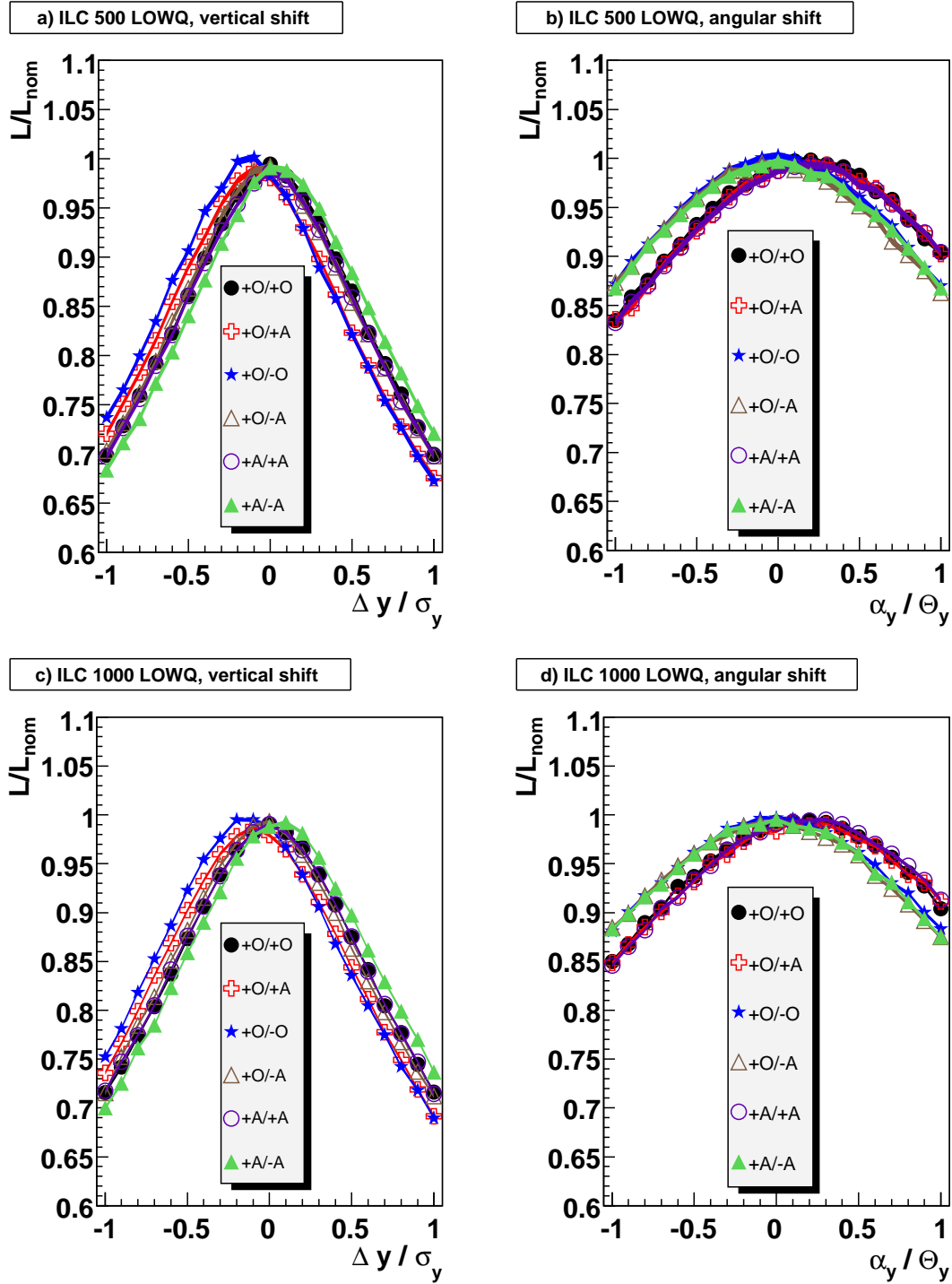


Figure 4: Offset followed by angle scans of the normalised luminosity for different combinations of vertical (O = offset (y-plane)) to angular (A = angle (y'-plane)) correlations leading to 6% luminosity growth. The angle scans have been performed for the maximum luminosity reached in the offset scan. Shown here is the low bunch charge option for 500 GeV (a and b) and 1000 GeV (c and d).

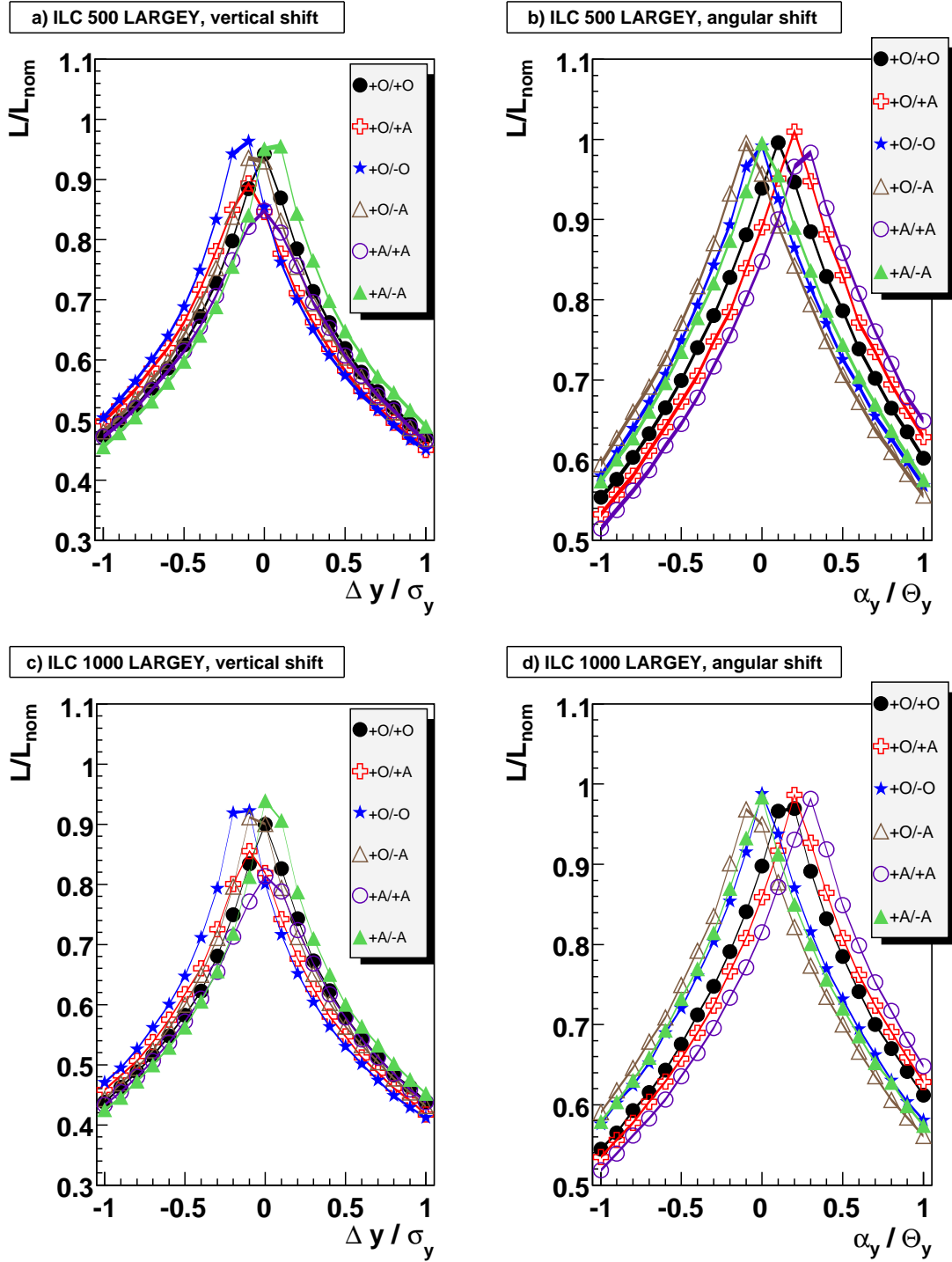


Figure 5: Offset followed by angle scans of the normalised luminosity for different combinations of vertical (O = offset (y-plane)) to angular (A = angle (y'-plane)) correlations leading to 6% luminosity growth. The angle scans have been performed for the maximum luminosity reached in the offset scan. Shown here is the option with increased vertical beam size for 500 GeV (a and b) and 1000 GeV (c and d).

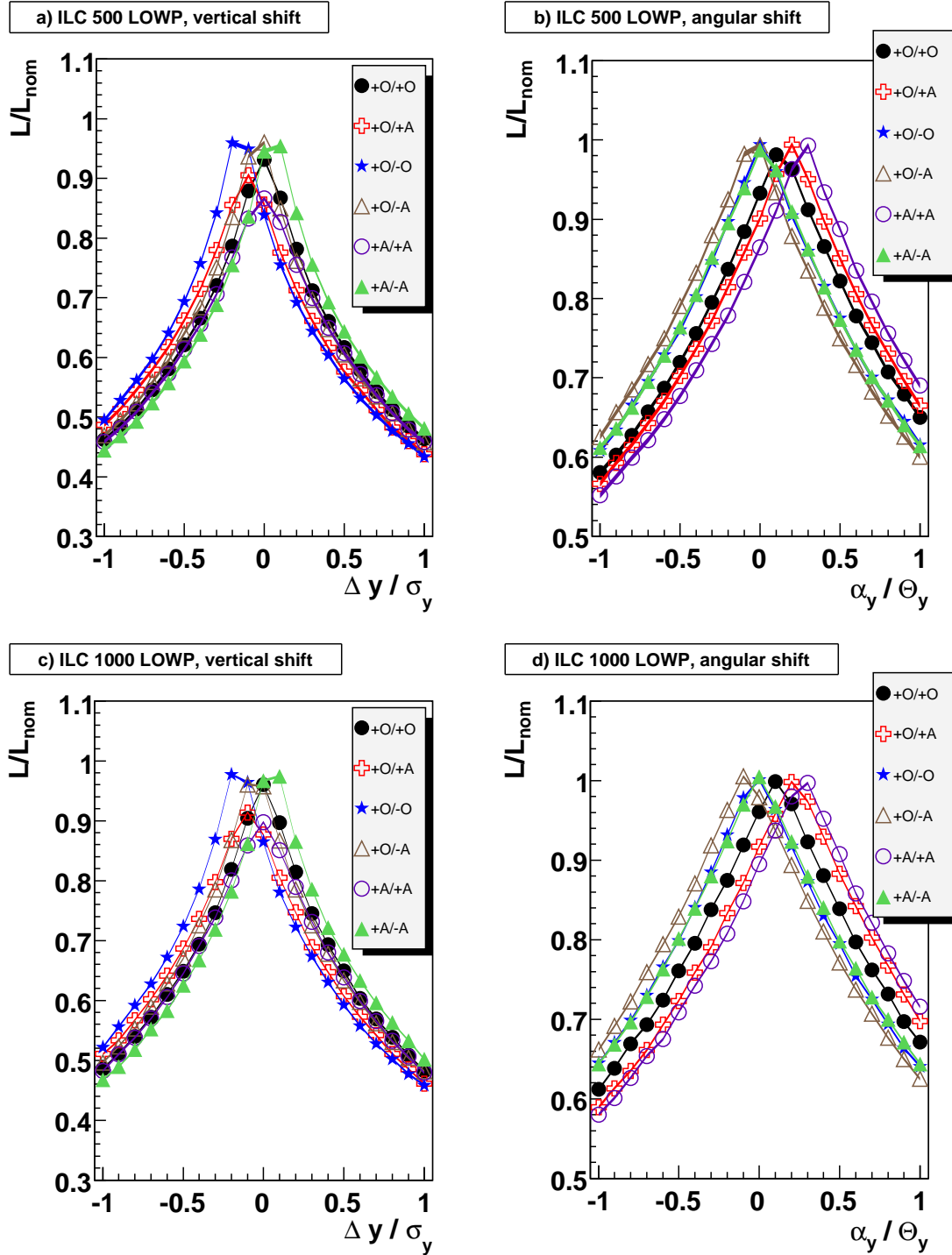


Figure 6: Offset followed by angle scans of the normalised luminosity for different combinations of vertical (O = offset (y-plane)) to angular (A = angle (y'-plane)) correlations leading to 6% luminosity growth. The angle scans have been performed for the maximum luminosity reached in the offset scan. Shown here is the low power (reduced number of bunches) option for 500 GeV (a and b) and 1000 GeV (c and d).

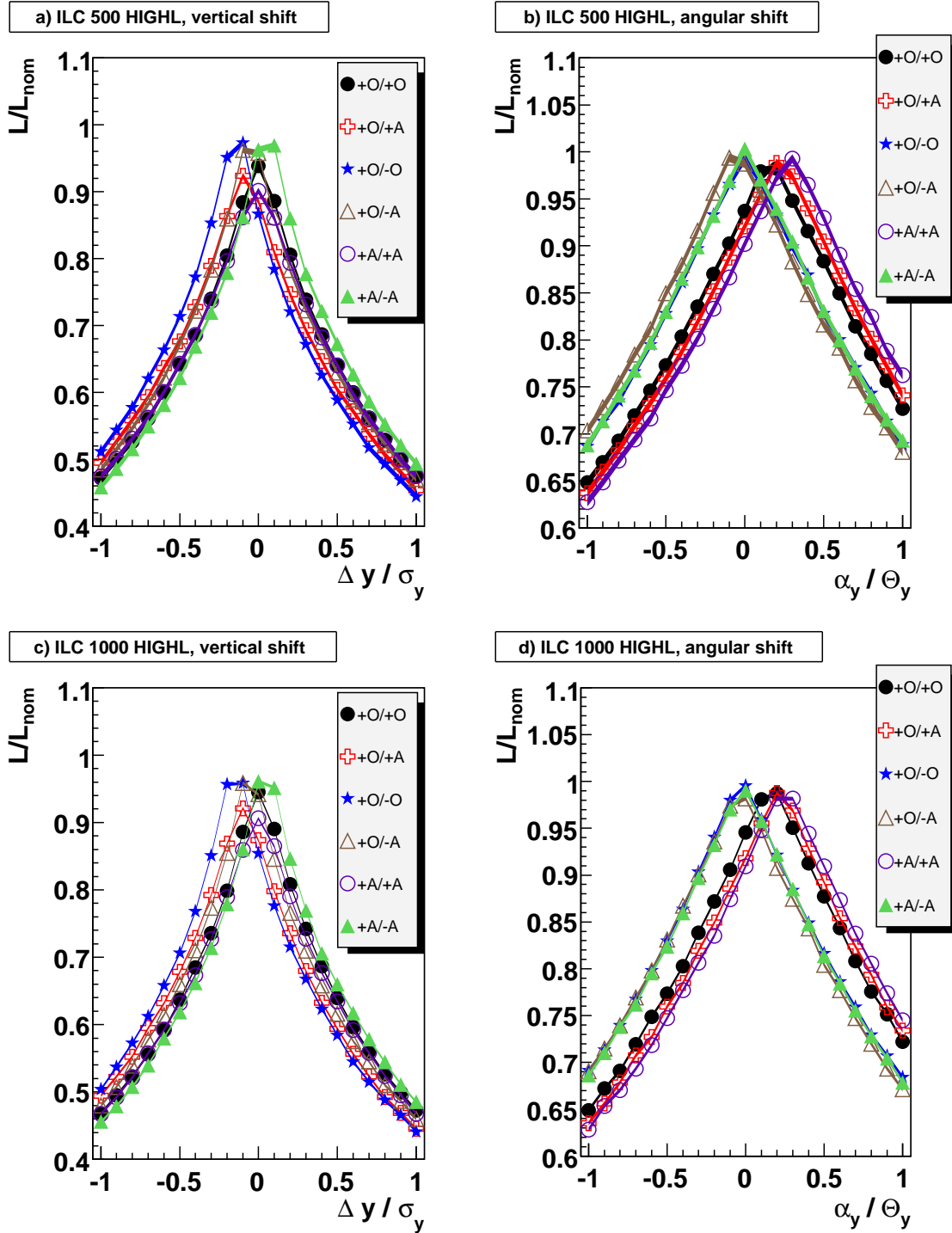


Figure 7: Offset followed by angle scans of the normalised luminosity for different combinations of vertical (O = offset (y-plane)) to angular (A = angle (y'-plane)) correlations leading to 6% luminosity growth. The angle scans have been performed for the maximum luminosity reached in the offset scan. Shown here is the high luminosity option for 500 GeV (a and b) and 1000 GeV (c and d).